Nanostructures and Optical Properties of Mesoporous Composite Nanofibers Containing CdS Quantum Dots

Weon-Sik Chae,[†] Sang-Wook Lee,[†] Myoung-Jin An,[†] Kyong-Hoon Choi,[†] Sik-Won Moon,[‡] Wang-Cheol Zin,[‡] Jin-Seung Jung,[§] and Yong-Rok Kim*,[†]

Photon Applied Functional Molecule Research Laboratory, Department of Chemistry, Yonsei University, Seoul 120-749, South Korea, Department of Materials Science and Engineering, Pohang University of Science and Technology, Pohang 790-784, South Korea, and Department of Chemistry, Kangnung National University, Kangnung 210-702, South Korea

Received April 20, 2005. Revised Manuscript Received September 6, 2005

Mesoporous silica nanofibers containing CdS quantum dots (QDs) were fabricated by the confined self-assembly of a lyotropic mesophase within the nanochannels of porous alumina. The resulting mesoporous nanofibers show unique internal mesostructures that depend on the size of the incorporated CdS QDs. Porous nanochannels of the composite nanofibers are shown to form a circularly wound assembly perpendicular to the long fiber axis with small QDs incorporated. As the diameter of the CdS QDs within the silica nanofibers increases, the circularly wound nanochannels become disordered. This unique mesoporous structure is further perturbed by increasing the amount of incorporated CdS QDs. The perturbed mesostructure inside the nanofibers results in an enhanced efficiency of nitrogen gas adsorption and spectral changes of the incorporated QD emissions. Such perturbed nanochannels inside the nanofibers can be utilized as a preferred mesostructure for adsorbing gas molecules and removing surface emission states of the CdS QDs.

Introduction

Because of the solid merits of cotrollable pore size, variable mesostructure, and functional composition,[1−3] mesoporous materials have attracted much attention in the fields of pure and applied sciences. By utilizing the channel-typed nanospace of mesoporous materials, unique chemical and physical properties have been introduced. The restricted mesoscopic environment that is provided by a nanochannel itself gives selective chemical reactions,[4] size-dependent molecular sieving,[5] and controlled energy properties.[6] To provide additional functions to siliceous mesoporous materials, researchers have tried to incorporate inorganic components such as transition metal ions and semiconductor nanocrystals within the framework and/or nanochannels of mesoporous silica materials.[3,7] Several studies on nanocomposite systems containing inorganic guest species have revealed interesting functional properties in the areas of catalysis,[8] magnetism,[9] and optics.[10]

* To whom correspondence should be addressed. Tel.: +82 (0)2 2123 2646. Fax: +82 (0)2 364 7050. E-mail: yrkim@yonsei.ac.kr.

[†] Yonsei University.

[‡] Pohang University of Science and Technology.

[§] Kangnung National University.

(1) (a) Zhao, D.; Feng, J.; Huo, Q.; Melosh, N.; Fredrickson, G. H.; Chmelka, B. F.; Stucky, G. D. *Science* **1998**, *279*, 548. (b) Kruk, M.; Jaroniec, M.; Sakamoto, Y.; Terasaki, O.; Ryoo, R.; Ko, C. H. *J. Phys. Chem. B* **2000**, *104*, 292. (c) Selvam, P.; Bhatia, S. K.; Sonwane, C. G. *Ind. Eng. Chem. Res.* **2001**, *40*, 3237.

(2) (a) Beck, J. S.; Vartuli, J. C.; Roth, W. J.; Leonowicz, M. E.; Kresge, C. T.; Schmitt, K. D.; Chu, C. T.-W.; Olson, D. H.; Sheppard, E. W.; McCullen, S. B.; Higgins, J. B.; Schlenker, J. L. *J. Am. Chem. Soc.* **1992**, *114*, 10834. (b) Soler-Illia, G. J. de A. A.; Sanchez, C.; Lebeau, B.; Patarin, J. *Chem. Rev.* **2002**, *102*, 4093.

(3) (a) Braun, P. V.; Osenar, P.; Stupp, S. I. *Nature* **1996**, *380*, 325. (b) Shen, S.; Tian, B.; Yu, C.; Xie, S.; Zhang, Z.; Tu, B.; Zhao, D. *Chem. Mater.* **2003**, *15*, 4046. (c) Yang, P.; Zhao, D.; Margolese, D. I.; Chmelka, B. F.; Stucky, G. D. *Nature* **1998**, *396*, 152. (d) MacLachlan, M. J.; Coombs, N.; Ozin, G. A. *Nature* **1999**, *397*, 681. (e) Trikalitis, P. N.; Kasthuri Rangan, K.; Bakas, T.; Kanatzidis, M. G. *Nature* **2001**, *410*, 671. (f) Jiao, F.; Bruce, P. G. *Angew. Chem., Int. Ed.* **2004**, *43*, 5958. (g) Lee, K.; Kim, Y.-H.; Han, S. B.; Kang, H.; Park, S.; Seo, W. S.; Park, J. T.; Kim, B.; Chang, S. *J. Am. Chem. Soc.* **2003**, *125*, 6844. (h) Riley, A. E.; Tolbert, S. H. *J. Am. Chem. Soc.* **2003**, *125*, 4551. (i) Choi, S. Y.; Mamak, M.; Coombs, N.; Chopra, N.; Ozin, G. A. *Adv. Funct. Mater.* **2004**, *14*, 335. (j) Trikalitis, P. N.; Bakas, T.; Kanatzidis, M. G. *J. Am. Chem. Soc.* **2005**, *127*, 3910.

(4) (a) Ying, J. Y.; Mehnert, C. P.; Wong, M. S. *Angew. Chem., Int. Ed.* 1999, *38*, 56. (b) Shouro, D.; Moriya, Y.; Nakajima, T.; Mishima, S. *Appl. Catal. A: Gen.* **2000**, 198, 275.

(5) (a) Kisler, J. M.; Dähler, A.; Stevens, G. W.; O'Connor, A. J. *Microporous Mesoporous Mater.* **2001**, *44*−*45*, 769. (b) McCool, B. A.; Hill, N.; DiCarlo, J.; DeSisto, W. J. *J. Membr. Sci.* **2003**, *218*, 55.

(6) (a) Srdanov, V. I.; Alxneit, I.; Stucky, G. D.; Reaves, D. M.; DenBaars, S. P. *J. Phys. Chem. B* 1998, *102*, 3341. (b) Xu, W.; Guo, H.; Akins, D. L. *J. Phys. Chem. B* **2001**, *105*, 1543. (c) Kim, Y.; Choi, J. R.; Yoon, M.; Furube, A.; Asahi, T.; Masuhara, H. *J. Phys. Chem. B* **2001**, *105*, 8513. (d) Scott, B. J.; Wirnsberger, G.; Stucky, G. D. *Chem. Mater.* **2001**, *13*, 3140. (e) Chae, W.-S.; Kim, Y.-R.; Jung, J.-S. *J. Phys. Chem. B* **2003**, *107*, 1585. (f) Brieler, F. J.; Grundmann, P.; Fröba, M.; Chen, L.; Klar, P. J.; Heimbrodt, W.; Nidda, H.-A. K.; Kurz, T.; Loidl, A. *J. Am. Chem. Soc.* **2004**, *126*, 797. (g) Itoh, T.; Yano, K.; Kajino, T.; Itoh, S.; Shibata, Y.; Mino, H.; Miyamoto, R.; Inada, Y.; Iwai, S.; Fukushima, Y. *J. Phys. Chem. B* **2004**, *108*, 13683. (h) Molenkamp, W. C.; Watanabe, M.; Miyata, H.; Tolbert, S. H. *J. Am. Chem. Soc.* **2004**, *126*, 4476. (i) Minoofar, P. N.; Dunn, B. S.; Zink, J. I. *J. Am. Chem. Soc.* **2005**, *127*, 2656.

(7) (a) Kim, J. M.; Kwak, J. H.; Jun, S.; Ryoo, R. *J. Phys. Chem.* **1995**, *99*, 16742. (b) Wu, S.; Han, Y.; Zou, Y.-C.; Song, J.-W.; Zhao, L.; Di, Y.; Liu, S.-Z.; Xiao, F.-S. *Chem. Mater.* **2004**, *16*, 486. (c) Zhu, H.; Pan, Z.; Chen, B.; Lee, B.; Mahurin, S. M.; Overbury, S. H.; Dai, S. *J. Phys. Chem. B* **2004**, *108*, 20038. (d) Chen, S.-Y.; Jang, L.-Y.; Cheng, S. *Chem. Mater.* **2004**, *16*, 4174. (e) Yang, X.; Han, Y.; Lin, K.; Tian, G.; Feng, Y.; Meng, X.; Di, Y.; Du, Y.; Zhang, Y.; Xiao, F.-S. *Chem. Commun.* **2004**, 2612. (f) Lin, W.; Frei, H. *J. Phys. Chem. B* **2005**, *109*, 4929. (g) Kónya, Z.; Puntes, V. F.; Kiricsi, I.; Zhu, J.; Ager, J. W., III; Ko, M. K.; Frei, H.; Alivisatos, P.; Somorjai, G. A. *Chem. Mater.* **2003**, *15*, 1242.

10.1021/cm050839j CCC: $30.25
Published on Web 10/13/2005

In other respects, the incorporated inorganic components sometimes work as additional structural defects in their mesoporous host frameworks. Therefore, the introduced defects can be a factor in inducing a modification of the intrinsic ordering of mesoporous nanochannels[11] that results in a variety of interesting macroscopic morphologies such as curved, spiral, gyroidal, and spheroidal shaped mesoporous materials.[12] In addition to the macroscopic ordering induced by guest incorporation, morphology fabrication controlled with nanodimensional parameters in films and fibers has also recently been investigated in the field of mesoporous materials.[13−19] The morphologies of nanosized films and fibers are structurally confined systems in one and two dimensions, respectively. In particular, mesoporous nanofiber that is a two-dimensionally (2D) confined system has recently been studied in terms of its fundamental interest for understanding confined mesoscopic self-assembly and the potential application of advanced functional nanomaterials.[14−19]

Mesoporous silica nanomaterials with a fiber morphology have been typically achieved using two different approaches: One is the direct mesoscopic self-assembly of surfactant and silica sol in acidic solution,[14−16] and the other is the confinement-induced mesoscopic self-assembly of surfactant and silica sol within a porous nanochannel template.[17−19] The internal mesostructures of the silica nanofibers could be controlled with the reaction parameters of composition, temperature, acidity, and aging time.[14−19] The resulting mesoporous nanofibers can be classified mainly according to two internal mesostructures: the nanochannel alignment parallel to the long fiber axis[14,15,17,18] and the circularly wound nanochannel alignment perpendicular to the long fiber axis.[15,16,18,19]

Mesoporous nanofibers with such unique nanochannel alignments can be utilized for more diverse applications (molecular catalysis, sensor, nonlinear optics, etc.) if a proper functional component is introduced into them. Regarding future applications, the advantages of mesoporous nanomaterials are their high reactivity and sensitivity, which are induced by their large surface areas. For a mesoporous nanofiber with an internal mesostructure of a parallelly aligned nanochannel assembly, external molecular species are easily accessible to the internal nanochannels because of the nanochannels that are open to the outside. On the other hand, a mesoporous nanofiber with a circularly wound nanochannel assembly typically has a closed channel system, so that external molecular species have somewhat hindered access to the inside of the internal nanochannels of such a nanofiber compared to an open channel system with straight nanopores. Therefore, as a facile route for the fabrication of advanced functional nanomaterials, the simultaneous control of internal mesostructure and functional properties is an important approach for developing dimensionally confined mesoporous nanomaterials.

In this study, as a new type of mesoporous nanocomposite, we have fabricated mesoporous silica nanofibers that are functionalized with semiconductor (CdS) quantum dots (QDs) by using a templating method with the cylindrical nanochannels of porous alumina. Depending on the diameter of the incorporated CdS QDs, the resulting mesoporous nanofibers exhibit interesting mesostructural transformations inside the nanofibers with simultaneous changes in gas adsorption behavior and CdS QD emissions.

Experimental Section

Chemicals. A porous alumina membrane with an average pore diameter of 200 ± 20 nm and a thickness of 60 μm was purchased from Whatman (Anodisc 13). The following chemicals were used as received: Pluronic F127 ($EO_{106}PO_{70}EO_{106}$; BASF Chemical Co.), tetraethyl orthosilicate (TEOS, 98%; Aldrich Chemical Co.), octadecyltrichlorosilane (>90%, Sigma-Aldrich Chemical Co.), cadmium nitrate tetrahydrate (98%; Kanto Chemical Co.), nitric acid (60%; Matsunden Chemical Co.), ethanol (>99.9%; Merck KGaA), and benzene (≥99.9%; Sigma-Aldrich Chemical Co.). H_2S gas was prepared by the dissolution of 1.6 g of sodium sulfide nonahydrate (≥92%; Kanto Chemical Co.) in 56 mL of 1 M hydrochloric acid (35%; Matsunden Chemical Co.).

Preparations. To facilitate the filling of the template by the lyotropic precursor solution, the nanochannel surface of the porous alumina template was modified with octadecyltrichlorosilane through refluxing in benzene for 10 h before infiltration of the lyotropic precursor solution. The lyotropic precursor solution

(8) (a) Trong On, D.; Desplantier-Giscard, D.; Danumah, C.; Kaliaguine, S. *Appl. Catal. A: Gen.* **2001**, *222*, 299. (b) Lee, C.-H.; Lin, T.-S.; Mou, C.-Y. *J. Phys. Chem. B* **2003**, *107*, 2543. (c) Kucœtrowski, P.; Chmielarz, L.; Dziembaj, R.; Cool, P.; Vansant, E. F. *J. Phys. Chem. A* **2005**, *109*, 330.

(9) (a) Jung, J.-S.; Chae, W.-S.; McIntyre, R. A.; Seip, C. T.; Wiley: J. B.; O'Connor, C. J. *Mater. Res. Bull.* **1999**, *34*, 1353. (b) Garcia, C.; Zhang, Y.; DiSalvo, F.; Wiesner, U. *Angew. Chem., Int. Ed.* **2003**, *42*, 1526. (c) Gross, A. F.; Diehl, M. R.; Beverly, K. C.; Richman, E. K.; Tolbert, S. H. *J. Phys. Chem. B* **2003**, *107*, 5475. (d) Haskouri, J. E.; Cabrera, S.; Gómez-García, C. J.; Guillem, C.; Latorre, J.; Beltrán, A.; Beltrán, D.; Marcos, M. D.; Amorrós, P. *Chem. Mater.* **2004**, *16*, 2805.

(10) (a) Bi, H.; Cai, W.; Shi, H.; Liu, X. *Chem. Phys. Lett.* **2002**, *357*, 249. (b) Pérez, M. D.; Otal, E.; Bilmes, S. A.; Soler-Illia, G. J. A. A.; Crepaldi, E. L.; Grosso, D.; Sanchez, C. *Langmuir* **2004**, *20*, 6879. (c) Gu, J.-L.; Shi, J.-L.; You, G.-J.; Xiong, L.-M.; Qian, S.-X.; Hua, Z.-L.; Chen, H.-R. *Adv. Mater.* **2005**, *17*, 557.

(11) (a) Zhang, W.; Glomski, B.; Pauly, T. R.; Pinnavaia, T. J. *Chem. Commun.* **1999**, 1803. (b) Bagshaw, S. A. *Chem. Commun.* **1999**, 1785.

(12) (a) Yuan, Z. Y.; Zhou, W.; Zhang, Z. L.; Liu, J. Q.; Wang, J. Z.; Li, H. X.; Peng, L. M. *Surf. Interface Anal.* **2001**, *32*, 193. (b) Yuan, Z.-Y.; Zhou, W.; Su, B.-L. *Chem. Phys. Lett.* **2002**, *361*, 307.

(13) (a) Ryoo, R.; Ko, C. H.; Cho, S. J.; Kim, J. M. *J. Phys. Chem. B* **1997**, *101*, 10610. (b) Zhao, D.; Yang, P.; Melosh, N.; Feng, J.; Chmelka, B. F.; Stucky, G. D. *Adv. Mater.* **1998**, *10*, 1380. (c) Doshi, D. A.; Huesing, N. K.; Lu, M.; Fan, H.; Lu, Y.; Simmons-Potter, K.; Potter, B. G., Jr.; Hurd, A. J.; Brinker, C. J. *Science* **2000**, *290*, 107. (d) Liu, N.; Assink, R. A.; Brinker, C. J. *Chem. Commun.* **2003**, 370.

(14) (a) Huo, Q. S.; Zhao, D. Y.; Feng, J. L.; Weston, K.; Buratto, S. K.; Stucky, G. D.; Schacht, S.; Schüth, F. *Adv. Mater.* **1997**, *9*, 974. (b) Che, S.; Liu, Z.; Ohsuna, T.; Sakamoto, K.; Terasaki, O.; Tatsumi, T. *Nature* **2004**, *429*, 281.

(15) (a) Wang, J.; Zhang, J.; Asoo, B. Y.; Stucky, G. D. *J. Am. Chem. Soc.* **2003**, *125*, 13966. (b) Wang, J.; Tsung, C.-K.; Hong, W.; Wu, Y.; Tang, J.; Stucky, G. D. *Chem. Mater.* **2004**, *16*, 5169.

(16) (a) Marlow, F.; Spliethoff, B.; Tesche, B.; Zhao, B. *Adv. Mater.* **2000**, *12*, 961. (b) Kleitz, F.; Marlow, F.; Stucky, G. D.; Schüth, F. *Chem. Mater.* **2001**, *13*, 3587. (c) Wang, J.; Tsung, C.-K. Hayward, R. C.; Wu, Y.; Stucky, G. D. *Angew. Chem., Int. Ed.* **2005**, *44*, 332.

(17) (a) Yamaguchi, A.; Uejo, F.; Yoda, T.; Uchida, T.; Tanamura, Y.; Yamashita, T.; Teramae, N. *Nat. Mater.* **2004**, *3*, 337. (b) Lu, Q.; Gao, F.; Komarneni, S.; Mallouk, T. E. *J. Am. Chem. Soc.* **2004**, *126*, 8650.

(18) (a) Yang, Z.; Niu, Z.; Cao, X.; Yang, Z.; Lu, Y.; Hu, Z.; Han, C. C. *Angew. Chem., Int. Ed.* **2003**, *42*, 4201. (b) Yao, B.; Fleming, D.; Morris, M. A.; Lawrence, S. E. *Chem. Mater.* **2004**, *16*, 4851. (c) Wang, D.; Kou, R.; Yang, Z.; He, J.; Yang, Z.; Lu, Y. *Chem. Commun.* **2005**, 166.

(19) (a) Chae, W.-S.; Lee, S.-W.; Im, S.-J.; Moon, S.-W.; Zin, W.-C.; Lee, J.-K.; Kim, Y.-R. *Chem. Commun.* **2004**, 2554. (b) Wu, Y.; Cheng, G.; Katsov, K.; Sides, S. W.; Wang, J.; Tang, J.; Fredrickson, G. H.; Moskovits, M.; Stucky, G. D. *Nat. Mater.* **2004**, *3*, 816.

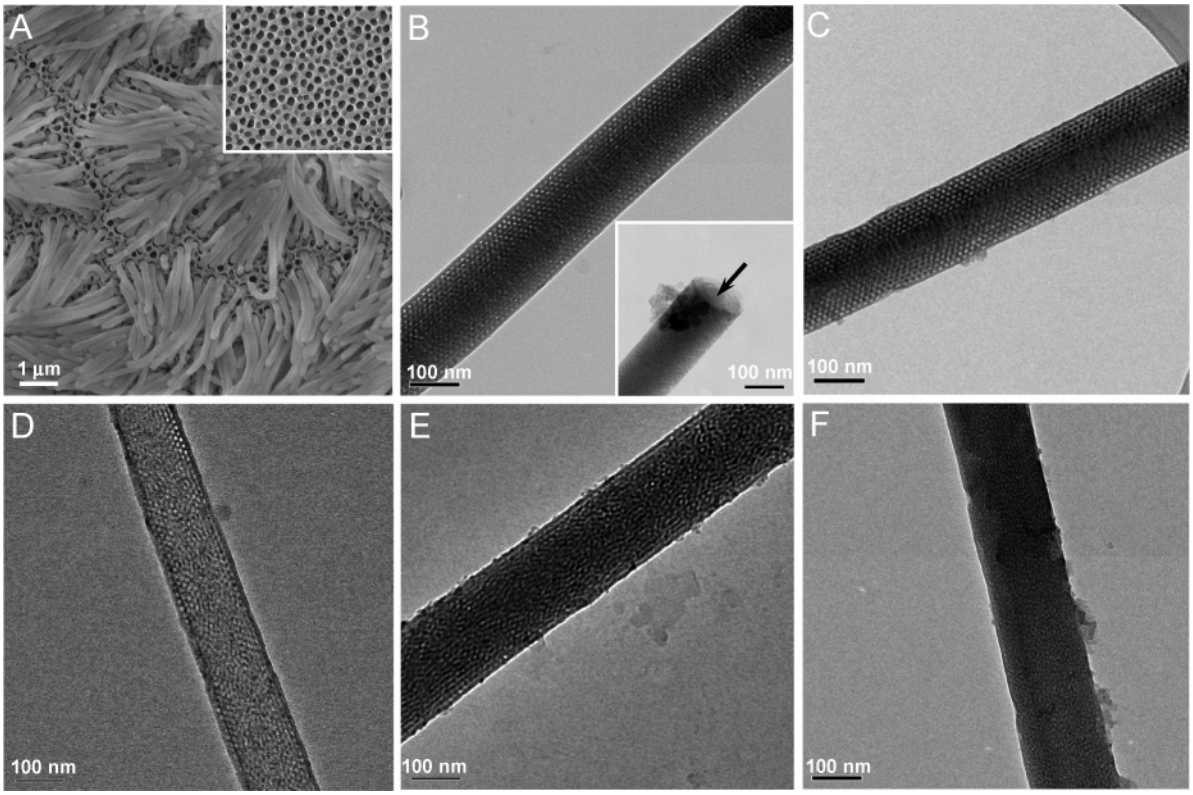

Figure 1. FE-SEM and TEM images of the mesoporous silica nanofibers containing CdS. (A) FE-SEM image of the mesoporous silica nanofiber with 1 mol % CdS. Inset: Representative FE-SEM image for an empty porous alumina template. TEM images are presented for the mesoporous silica nanofibers with the different loadings of CdS: (B) 1, (C) 3, (D) 5, (E) 10, and (F) 15 mol %. The inset of B is an image obtained on the cross-sectional part of a mesoporous nanofiber containing 1 mol % of CdS. These single mesoporous nanofibers were obtained after complete removal of porous alumina templates by a 1 M NaOH solution.

consisted of silica and cadmium precursors and the triblock copolymer Pluronic F127 in ethanol: 1 g of Pluronic F127 was homogeneously mixed with 2.1 g of TEOS, 0.03 g of cadmium nitrate tetrahydrate, and 0.54 g of 0.3 M nitric acid in 2.3 g of ethanol. The composition of this lyotropic precursor solution was 1 mol of TEOS/0.01 mol of Cd(II)/0.00008 mol of Pluronic F127/5 mol of ethanol. To investigate structural and optical properties, several lyotropic precursor solutions containing various molar ratios of Cd to TEOS (1, 3, 5, 10, and 15 mol %) were used for the infiltration within porous alumina templates. The porous alumina templates were dipped into the respective lyotropic precursor solutions, which slowly stirred for 12 h so that the porous alumina channels would be completely filled with the precursor solutions. The filled porous alumina membranes were then allowed to undergo gelation at 60 °C for 12 h. The resulting porous alumina membranes including the lyotropic supramolecular precursors were exposed to excess H_2S gas (20 mL) for 10 h, which immediately resulted in a membrane with the characteristic yellow color of CdS. Some of the bulk CdS that remained deposited on the membrane surface was removed and then subjected to calcination at 350 °C for 2 h to remove the Pluronic F127 organic template molecules incorporated in the mesoporous composite nanofibers (Supporting Information, Figure S1). After the complete removal of the porous alumina template with 1 M sodium hydroxide, mesoporous silica nanofibers that contained CdS QDs could easily be obtained.

Instrumentations. The mesoporous composite nanofibers were studied with a field-emission scanning electron microscope (FE-SEM, JEOL JSM-6700F), a transmission electron microscope (TEM, JEOL 3010), a nitrogen adsorption analyzer (Micromeritics ASAP-2010), a diffuse reflectance spectrophotometer (Jasco V-550) equipped with an integrating sphere (Jasco ISV-469), and a fluorescence spectrophotometer (Hitachi F-4500). Small-angle X-ray scattering measurements were performed in transmission mode with synchrotron radiation at the 3C2 X-ray beam ($\lambda = 0.1542$ nm) line at Pohang Accelerator Laboratory (POSTECH, Pohang, South Korea). The X-ray beam was vertically aligned to the plane of porous alumina membranes that contained the mesoporous composite nanofibers.

Results and Discussion

Figure 1 shows FE-SEM and TEM images of the CdS-incorporated mesoporous silica nanofibers that were fabricated using the above-described templating method within the cylindrical nanochannels of porous alumina. The mesoporous composite nanofibers containing CdS QDs are shown to be almost filled within the nanochannels of porous alumina template (Figure 1A). After the complete removal of the porous alumina template with 1 M sodium hydroxide, the resulting composites of mesoporous nanomaterials clearly represent the fiber morphology, as shown in Figure 1B−F. The single composite nanofiber containing a low content (1 mol %) of CdS shows a unique mesoporous structure in which pores with an average diameter of ~6 nm are shown to be hexagonally arrayed in a side view. Interestingly, it is noteworthy that an onionlike concentric ring is observed in the cross section of the composite nanofiber (marked by an arrow in the inset of Figure 1B). These mesostructural features indicate that the observed mesoporous nanochannels inside the nanofiber have the unique porous structure of the circularly wound nanochannel alignment perpendicular to the long fiber axis, as similarly reported previously.[15,16,18,19] This novel structural feature is still observed in the mesoporous composite nanofiber containing an increased content (3 mol

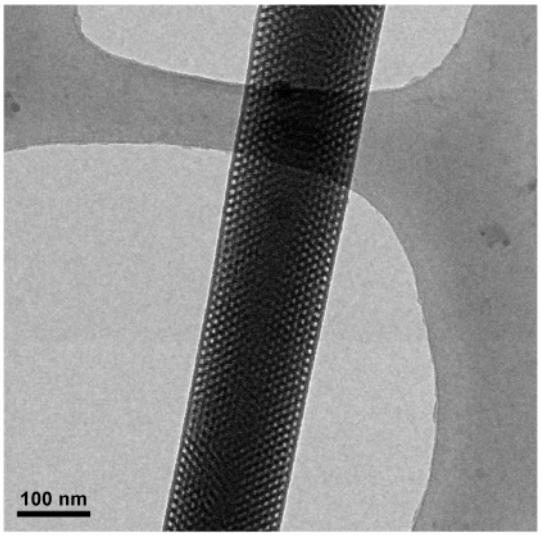

Figure 2. TEM image of the mesoporous silica nanofiber containing only Cd(II) ions of 10 mol %.

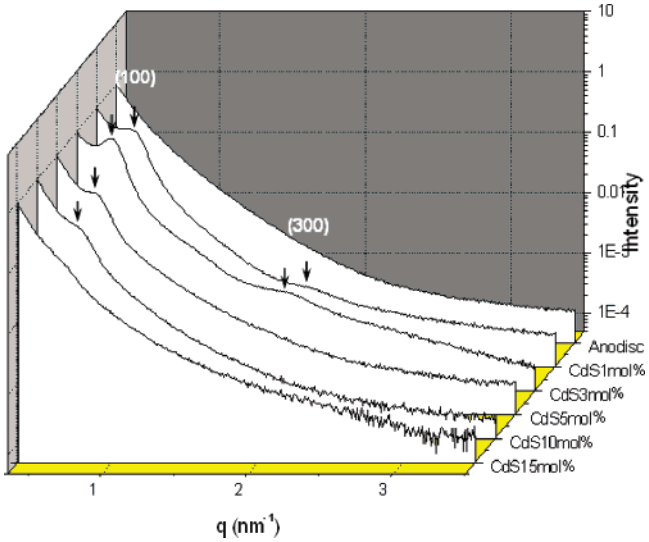

Figure 3. X-ray diffraction patterns in the small-angle region for mesoporous silica nanofibers with various loadings of CdS. An X-ray diffraction pattern for an empty porous alumina (Anodisc) is also presented for comparison.

%) of CdS component. As the loading of CdS is further increased through 5 to 10 mol %, the characteristic mesostructure of the composite nanofibers is partially deformed from the central region (Figure 1D) and subsequently becomes disordered as a wormlike network (Figure 1E). For the composite nanofiber with the higher CdS content of 15 mol %, even the wormlike nanochannel network disappears. Nevertheless, the mesoporous composite nanomaterials still preserve their fiber morphology, regardless of the transformations of their internal mesostructures.

From the previous studies on bulk mesoporous materials, it has been suggested that the incorporation of inorganic guest species perturbs the formation of the mesoporous silica host.[11] A weak strain that is imposed by external doping with a sufficiently dilute concentration within the silica wall framework can induce a slight deformation of its mesoporous structure, which results in various macroscopic shapes of the mesoporous material, such as curved, spiral, gyroidal, and spheroidal shapes.[12] In this study, the mesoporous structures inside the nanofibers are shown to be highly dependent on the loading of the CdS component. To understand the involved transformation mechanism, a further study was performed with the mesoporous nanofiber with a loading of 10 mol %. Figure 2shows the TEM image for the mesoporous silica nanofiber containing 10 mol % of Cd(II) ions. The image was obtained for the specimen just before its exposure to H_2S gas, i.e., before the formation of CdS. It is notable that the unique well-organized mesostructure is still observed for this nanofiber, whereas the mesoporous composite nanofiber after exposure to H_2S gas exhibits the wormlike mesostructure as shown in Figure 1E. On the basis of these results, it is considered that the Cd(II) species incorporated within silica wall framework are not responsible for the deformation of the mesostructure, but rather that the formation of CdS QDs is responsible for this deformation. The identification of the incorporated CdS QDs existing within the mesoporous nanofibers is fully discussed in a later section. When the calcination process is performed at higher temperature (450 °C), the oxidation of the doped CdS QDs induces the deformation of the unique mesostructure. However, this oxidation effect on the structural deformation was experimentally found to be negligible for these mesoporous composite nanofibers calcined at 350 °C (see Supporting Information). Such deformation of the mesostructure can change the macroscopic fiber shape of the mesoporous material. However, any prominent shape changes were not observed in the macroscopic view after the formation of CdS nanocrystals within the mesoporous nanofibers. The reason is expected to be a spatial confinement effect within the 2D confined nanospace, i.e., the cylindrical nanochannels of the porous alumina template. This expectation can be supported by the following observation: As shown in Figure 1D, the relatively well-organized mesostructure still exists in the outer surface region of the mesoporous nanofiber, even though the unique mesoporous structure is disordered in the central region.

Figure 3shows the X-ray diffraction patterns in the small-angle region for CdS-incorporated mesoporous silica nanofibers that are confined within porous alumina membranes. The mesoporous silica nanofibers containing low contents (1 and 3 mol %) of CdS exhibit two diffraction peaks at 0.59 and 1.77 nm^{-1}. These scattering peaks are well correlated to the (100) and (300) Miller planes of a lamellar structure ($d_{100} = 10.64$ nm). Because the X-ray beam used was vertically irradiated on the plane of the composite membranes (transmission detection mode), such diffractional scatterings can be assigned to the pseudo-lamellar structure of the onionlike concentric ring assembly of the mesoporous nanochannels. In particular, it can be seen that even-order diffractions corresponding to the (200) and (400) planes are not clearly observed in these composite systems. According to the theory for an ideal two-phase alternating lamellar system,[20] it is expected that Bragg diffraction peaks occur at the series of q values satisfying $q = 2\pi n/d$ and that the intensity of the nth-order peak is proportional to $\sin^2(\pi n\phi_A)/n^2$, where ϕ_A ($= d_A/d$) is the volume fraction of one (A)

(20) Roe, R. J. *Methods of X-ray and Neutron Scattering in Polymer Science*; Oxford University Press: New York, 2000.

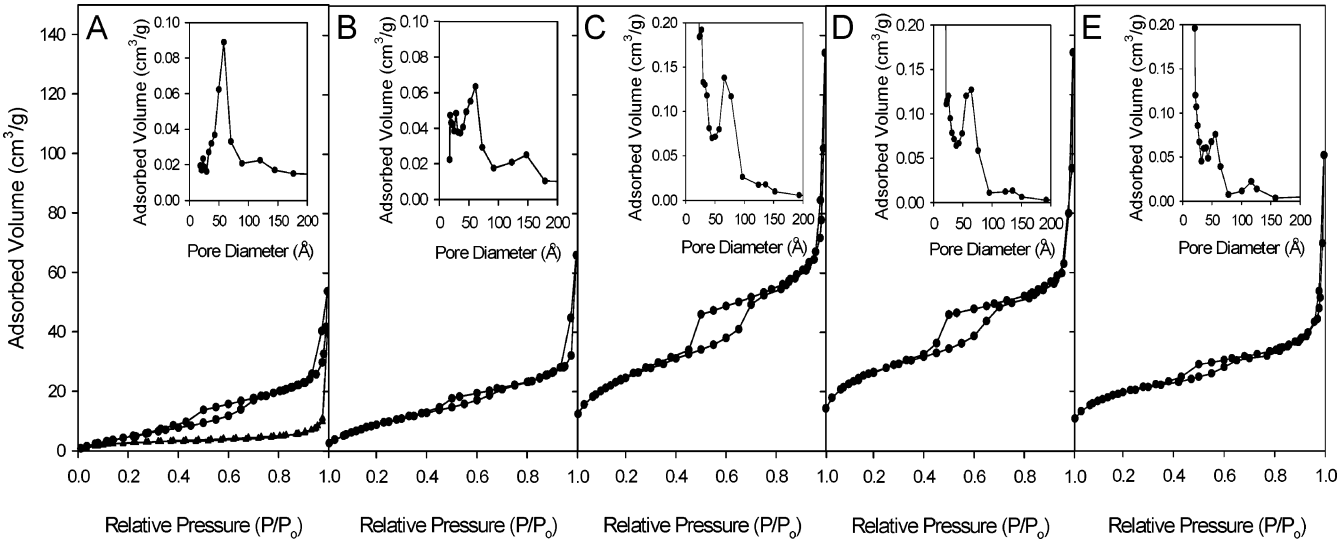

Figure 4. Nitrogen gas adsorption−desorption isotherms of mesoporous silica nanofibers with different loadings of CdS: (A) 1, (B) 3, (C) 5, (D) 10, and (E) 15 mol %. The insets are pore size distributions estimated by applying the Barrett−Joyner−Halenda (BJH) method to the adsorption branches of the corresponding mesoporous nanofibers.

phase. Therefore, one can expect that, when the volumes of the two phases are equal, all even-order peaks are reduced to zero intensity. This absence of even-order peaks in these mesoporous composite nanofibers implies that the pseudo-lamellar structure has similar phase volumes for both the silica framework and the void nanochannel.

The mesoporous silica nanofibers containing the increased loadings (5 and 10 mol %) of CdS show only a diffraction peak from the (100) plane, whereas the diffraction peak corresponding to the (300) plane is largely suppressed in intensity. This large suppression of the high-order peak implies a loss of mesostructural ordering. As the CdS loading increases further to 15 mol %, even the diffraction peak from the (100) plane is largely suppressed, implying a destruction of the internal mesoporous structure. Such a trend in the results is well correlated with the mesostructural transformation observed in the TEM study.

Figure 4 shows the nitrogen gas adsorption−desorption isotherms for CdS-incorporated mesoporous silica nanofibers that are confined within porous alumina templates. Compared to the empty porous alumina membrane that shows a simple Langmuir-type adsorption behavior, all composite nanofibers present unique adsorption−desorption hysteresis loops in the range of $0.4-0.7P/P_o$. Such an adsorption behavior is typical of mesoporous materials,[21] and it can be attributed to the mesoporous composite nanofibers confined within porous alumina template. In contrast to the empty porous alumina membrane, the porous alumina membranes filled with mesoporous composite nanofibers exhibit relatively high Brunauer−Emmett−Teller (BET) surface areas and large pore volumes, even though these composite membranes include a massive weight contribution (at least more than 90 wt %) by the porous alumina. In general, the BET surface area and pore volume gradually increase as the loading of CdS increases up to 10 mol %. The estimated major pore diameters are ~6 nm for the mesoporous composite nanofibers with CdS contents of 1−10 mol % (Table 1).

Table 1. Adsorption Parameters and Diameters of the Incorporated CdS QDs for the Mesoporous Composite Nanofiber Membranes

sample	BET surface area (m^2/g)	pore volume (cm^3/g)	pore size[a] (nm)	QD diameter[b] (nm)
empty porous alumina	9.4	0.015	−	−
1 mol % CdS composite	25.1	0.046	6	3.2
3 mol % CdS composite	38.6	0.050	6	3.8
5 mol % CdS composite	85.8	0.111	6	5.3
10 mol % CdS composite	92.6	0.147	6	>6
15 mol % CdS composite	68.3	0.074	5	>6

[a] Pore sizes are estimated by applying the BJH method to the adsorption branches of the corresponding mesoporous composite nanofibers. [b] Diameters of the incorporated CdS QDs were estimated from the absorption onsets of the corresponding mesoporous composite nanofibers by applying the modified effective mass approximation, as proposed in a previous study.[24]

From the nitrogen gas adsorption analysis, it is noticed that both the BET surface area and pore volume are abruptly increased by at least a factor of 2 as the CdS loading increases from 3 to 5 mol %, even though the pore size remains constant. Furthermore, the contribution of nanopores with a pore size of less than 3 nm is distinctly enhanced for mesoporous composite nanofibers with CdS contents of 5−15 mol % compared to composite nanofibers containing CdS contents lower than 5 mol % (insets of Figure 4). Interestingly, the change of this adsorption behavior is simultaneously accompanied with the mesostructural change inside the nanofiber, as shown in Figure 1: As the CdS loading increases from 3 to 5 mol %, the mesostructural deformation, i.e., the randomization of the circularly wound nanochannels, is observed from the TEM images. Such correlation in the mesostructural changes from the TEM images and the adsorption behavior indicates that the mesoporous composite nanofibers containing the CdS loadings of 5 and 10 mol % have better mesostructures, because of the randomly oriented nanochannels and the increased contribution of nanopores, for the absorption/desorption efficiency of nitrogen gas molecules. With further loading up to 15 mol % of CdS content, the overall reductions are observed in BET surface area, pore volume, and pore size,

(21) (a) Sing, K. S. W.; Everett, D. H.; Haul, R. A. W.; Moscou, L.; Pierotti, R. A.; Rouquerol, J.; Siemieniewska, T. *Pure Appl. Chem.* **1985**, *57*, 603. (b) Kruk, M.; Jaroniec, M. *Chem. Mater.* **2001**, *13*, 3169.

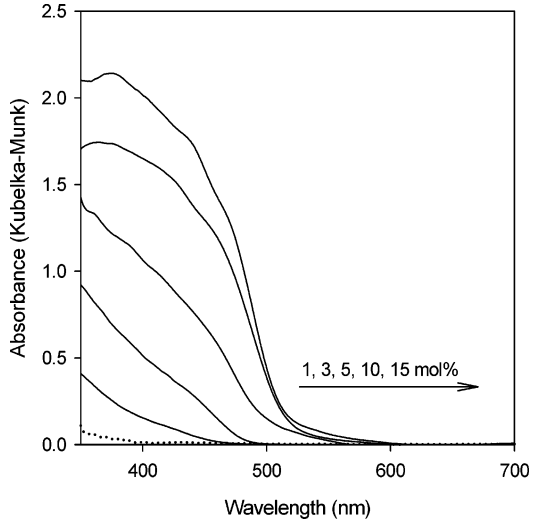

Figure 5. Absorption spectra of mesoporous silica nanofibers containing different loadings of CdS. The absorption spectrum for an empty porous alumina is also presented (dotted line). The absorption spectra were obtained by applying a Kubelka−Munk function to the diffuse reflectance spectra.

which are possibly due to the collapse of the unique mesoporous structure inside the nanofiber.

The resulting mesoporous composite nanofibers present the typical band-to-band absorption in the visible spectral region because of the incorporated CdS QDs, whereas the empty porous alumina template does not show any prominent optical absorption in the similar spectral region (Figure 5). It is noteworthy that the absorption onset is gradually shifted to longer wavelength region with increasing the CdS loading and it consequently approaches to the band-gap absorption (∼520 nm) of bulk CdS.[22] Such spectral shift can be induced by the quantum size effect of the incorporated semiconductor component:[22−24] Increased content of CdS typically generates larger size of QD within silica matrix.[25] Based on the quantum size effect,[24] the estimated diameter of the incorporated CdS QDs is shown to be linearly increased with increasing the loadings (Table 1). As shown in the representative high-resolution TEM (HR-TEM) images for the mesoporous composite nanofiber containing 3 and 10 mol % CdS (Figure 6), the diameters of the incorporated CdS QDs are shown to be 3−4 and 5−8 nm, respectively, of which diameters are reasonably comparable to those values estimated from the absorption spectra. After a complete removal of the mesoporous silica matrix, it is also proved that the diameter of the liberated CdS QDs have the similar diameter with that incorporated within the mesoporous silica matrix (Supporting Information, Figure S4).

Figure 7 shows the emission spectra for the mesoporous composite nanofibers, which exhibits the largely Stokes-shifted emissions as well as the band-edge emission. In general, photoexcited charge carriers (electron and hole) in

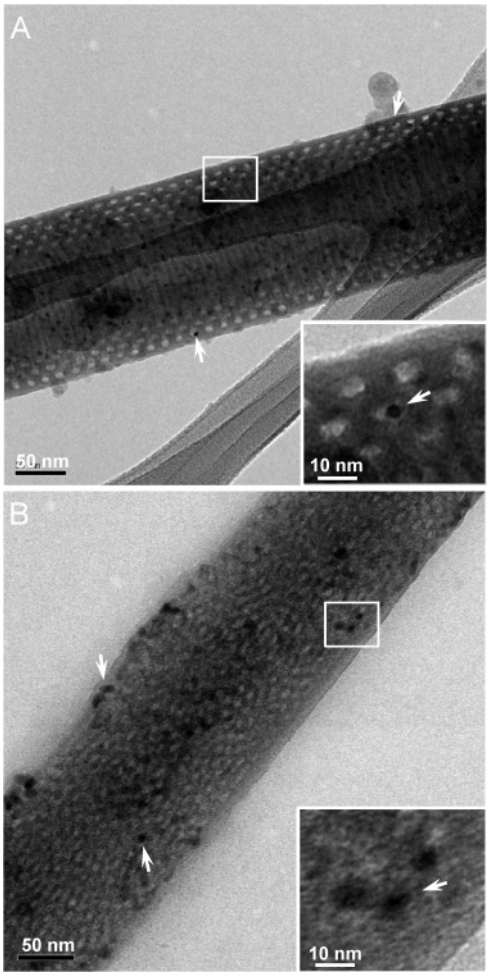

Figure 6. HR-TEM images of mesoporous silica nanofibers containing different CdS loadings of (A) 3 and (B) 10 mol %. The insets are magnified TEM images for the corresponding samples.

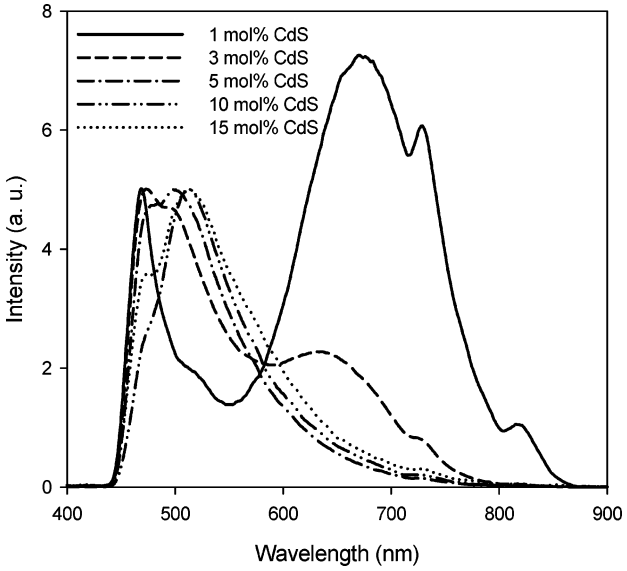

Figure 7. Emission spectra of mesoporous silica nanofibers with different loadings of CdS. The excitation wavelength for the emission spectra was 430 nm.

semiconductor recombine each other through several recombination processes such as direct band-to-band coupling and/or shallowly/deeply trapped potential states.[26] Defect sites existing on the surface of semiconductor nanocrystal typically provide deeply trapped potential states which induce such

(22) Rossetti, R.; Hull, R.; Gibson, J. M.; Brus, L. E. *J. Chem. Phys*. **1985**, *82*, 552.
(23) (a) Wang, Y.; Herron, N. *J. Phys. Chem*. **1991**, *95*, 525. (b) Alivisatos, A. P. *J. Phys. Chem*. **1996**, *100*, 13226.
(24) Nosaka, Y. *J. Phys. Chem*. **1991**, *95*, 5054.
(25) (a) Wang, Y.; Herron, N. *J. Phys. Chem*. **1987**, *91*, 257. (b) Parvathy, N. N.; Pajonk, G. M.; Rao, A. V. *Nanostruct. Mater*. **1997**, *8*, 929. (c) Bhattacharjee, B.; Bera, S. K.; Ganguli, D.; Chaudhuri, S.; Pal, A. K. *Eur. Phys. J. B* **2003**, *31*, 3.

largely Stokes-shifted emissions.[27,28] From the emission spectra, two apparent optical properties are observed depending on the loading amount of the doped CdS: One is the band-edge emission shift, which is red-shifted with increasing the amount of the doped CdS. The other is the intensity change of the largely Stokes-shifted emission. The former band-edge emission shift which is consistent with the absorption onset shift implies that the observed band-edge emission shift is originated from the quantum confinement effect of photoexcited charge carriers within the doped CdS QDs. The intensity of the largely Stokes-shifted emissions are decreased when the CdS loading increases from 1 to 3 mol %, which is further suppressed for the composite nanofibers with the higher loadings (5, 10, and 15 mol %). The intensity change of the largely Stokes-shifted emissions is believed to be due to the density change of surface defective emission states, and this density change of surface defect states possibly comes from the diameter and/or the surface chemical coupling of the doped CdS QDs. As the nanocrystal size increases, surface area generally decreases, and then the carriers' recombination process through these surface defect states can also be reduced.[29] Therefore, the relatively reduced surface defect emission compared with the band-edge emission is generally observed on larger semiconductor nanocrystals.[30] The other possible factor for the reduced density of surface defect states is surface chemical couplings between the doped CdS QDs and their surrounding silica matrix. It was previously reported that CdS nanoparticles encapsulated within porous silica matrix were chemically coupled with the surrounding silica.[31] They suggested that the excited-state property of the incorporated CdS nanoparticles could be affected by the chemical bonding with the silica. In this study, the CdS QDs are incorporated within the mesoporous silica, therefore, the surface chemical coupling is unavoidable in these composite nanofibers.

From the TEM images, the CdS QDs are shown to be well dispersed within the mesoporous nanofiber (Figure 6). Interestingly, some of the 3−4 nm QDs existing inside nanochannels have open surface which is not tightly coupled to mesoporous wall framework (indicated by arrows in Figure 6A). On the other hand, for the mesoporous composite nanofiber with the 10 mol % CdS loading, the incorporated CdS QDs appear to be well enclosed with the disordered wall framework, as indicated by arrows in Figure 6B. In this case, the density of surface defect states seems to be reduced by the surface couplings with the siliceous wall framework to a greater extent than with the 3 mol % CdS-incorporated nanofiber. Although the exact estimation of the degree of surface chemical coupling is somewhat difficult for these unique mesostructured composite nanomaterials, it can be plausibly suggested that this stronger surface chemical coupling works as a contributing factor for the large suppression of the surface defect emissions for the composite nanofibers with the high loadings of CdS in addition to the surface area effect induced by the size of the QDs.

Therefore, these mesoporous composite nanofibers containing high CdS loadings of 5−10 mol % can be utilized as optical materials, including photocatalysts, by applying a specific band energy induced by the incorporated CdS QDs, which is a response to the adsorbed molecular species within the mesoporous composite nanofibers.

Conclusions

In this study, we have fabricated mesoporous composite nanofibers containing CdS QDs, which were achieved by the confined self-assembly of a lyotropic mesophase within the cylindrical nanochannels of porous alumina. The resulting mesoporous composite nanofibers exhibit a unique transformation of the internal mesoporous structures that depends on the loading of CdS. This mesostructural change simultaneously induces changes in the optical properties of absorption and emission spectra. The concept of such interactive control of dimensionally confined nanomaterials will hopefully provide a facile route for developing advanced functional nanomaterials.

Acknowledgment. This work was financially supported by a National R&D Project for Nano-Science and Technology (Grant M1-0214-00-0021), a National Research Laboratory program (Grant M1-0302-00-0027) and a Yonsei Center for Studies on Intelligent Biomimic Molecular Systems. J.S.J. acknowledges a grant (RTI05-01-02) from MOCIE. We are grateful for the instrumental support from the equipment facility of CRM-KOSEF.

Supporting Information Available: Thermogravimetric analysis data for all composite nanofibers, absorption and emission spectra and TEM images for the 3 mol % CdS doped nanofibers after calcination at different temperatures, and TEM images and electron diffraction pattern of the liberated CdS QDs after the complete removal of the mesoporous silica matrix. These materials are available free of charge via the Internet at http://pubs.acs.org.

CM050839J

(26) Gaponenko, S. V. *Optical Properties of Semiconductor Nanocrystals*; Cambridge University Press: New York, 1998.
(27) (a) Chestnoy, N.; Harris, T. D.; Hull, R.; Brus, L. E. *J. Phys. Chem.* **1986**, *90*, 3393. (b) O'Neil, M.; Marohn, J.; McLendon, G. *J. Phys. Chem.* **1990**, *94*, 4356. (c) Wang, Y.; Suna, A.; McHugh, J.; Hilinski, E. F.; Lucas, P. A.; Johnson, R. D. *J. Chem. Phys.* **1990**, *92*, 6927. (d) Wu, F.; Zhang, J. Z.; Kho, R.; Mehra, R. K. *Chem. Phys. Lett.* **2000**, *330*, 237.
(28) (a) Spanhel, L.; Haase, M.; Weller, H.; Henglein, A. *J. Am. Chem. Soc.* **1987**, *109*, 5649. (b) Peng, X. G.; Wilson, T. E.; Alivisatos, A. P.; Schultz, P. G. *Angew. Chem., Int. Ed.* **1997**, *36*, 145. (c) Gao, M. Kirstein, S.; Möhwald, H.; Rogach, A. L.; Kornowski, A.; Eychmüller, A.; Weller, H. *J. Phys. Chem. B* **1998**, *102*, 8360. (d) Rogach, A. L.; Kornowski, A.; Gao, M.; Eychmüller, A.; Weller, H. *J. Phys. Chem. B* **1999**, *103*, 3065.
(29) (a) Bhargava, R. N.; Gallagher, D.; Hong, X.; Nurmikko, A. *Phys. Rev. Lett.* **1994**, *72*, 146. (b) Chen, W.; Xu, Y.; Lin, Z.; Wang, Z.; Lin, L. *Solid State Commun.* **1998**, *105*, 129.
(30) (a) Murray, C. B.; Norris, D. J.; Bawendi, M. G. *J. Am. Chem. Soc.* **1993**, *115*, 8706. (b) Landes, C. F.; Braun, M.; El-Sayed, M. A. *J. Phys. Chem. B* **2001**, *105*, 10554. (c) Krishnadasan, S.; Tovilla, J.; Vilar, R.; deMello, A. J.; deMello, J. C. *J. Mater. Chem.* **2004**, *14*, 2655.
(31) (a) Herron, N.; Wang, Y.; Eddy, M. M.; Stucky, G. D.; Cox, D. E.; Moller, K.; Bein, T. *J. Am. Chem. Soc.* **1989**, *111*, 530. (b) Chae, W.-S.; Ko, J.-H.; Hwang, I.-W.; Kim, Y.-R. *Chem. Phys. Lett.* **2002**, *365*, 49.